Effects of Surface Orientation and Body Thickness on the Performance of III-V Ultrathin-Body nMOSFETs

Tsung-Hsing Yu
Phorsight Company
e-mail: songsingyu@gmail.com

***Abstract*—This work proposes a theoretical investigation of different channel materials, (111) and (100) two surface orientations, and body thickness effects on the performance of III-V ultrathin-body FETs. A simulation methodology is presented based on in-house empirical tight-binding and top-of-the-barrier models. Simulation results indicate that (100) ballistic performance, in general, is better than (111) performance. Moreover, a (100) InP FET obtains the greatest Ion due to its high injection velocity and flattened energy dispersion. Also, a thicker InP ultrathin-body benefits to its on-state current while a thinner GaSb FET yields better performance.**

Keywords—tight-binding; top-of-the-barrier; III-V; ultrathin-body; nMOSFETs; injection velocity; density of states

I. INTRODUCTION

A III-V semiconductor thin body FET has been recognized as one of the most promising high mobility channel candidates for ultra-scaled MOSFETs [1] due to its lighter electron and hole effective masses compared to conventional silicon devices. The lighter effective mass, however, also results in smaller density of states (DOS) in III-V MOSFETs. Hence the on-state current, Ion, is limited by the smaller charge density arising from the bottleneck of DOS.

Recent studies have shown that GaSb double-gate ultra-thin-body (DG-UTB) with (100) or (111) surfaces could outperform Si by 40% under Vd=0.8v and EOT=0.5nm [2]. However, the benefit of the DOS improvement in GaSb DG-UTB was compensated by an increase of phonon scattering and therefore no significant performance improvement was observed [3]. On the other hand, Ref. [4] found that the on-state current of GaSb DG-UTB in (100) surface generally exhibited better performance than that in (111) surface. These studies also revealed that III-V materials with (111) surface orientation and a small Γ-L energy separation such as GaAs and GaSb UTB FETs could improve the DOS bottleneck. This is because the confined L-valley contributes additional bands to the Brillouin zone center in additional to Γ-valley [2-3].

From a device performance standpoint, it is desirable to use high DOS channel materials to improve on-state current. Therefore the band structure engineering such as the modulation of surface orientation and combined with various body thickness values could be utilized to improve the DOS and injection velocity in III-V DG-UTB FETs. Hence this paper intends to provide a physical understanding of the surface orientation and body thickness effects on the ballistic performance of III-V DG-UTB nMOSFETs. Also it further discusses how these two important factors, DOS and injection velocity, play a role on determining the ballistic performance.

II. SIMULATION METHODOLOGY AND MODEL VALIDATION

A DG-UTB structure is used in this study and its body thickness values cover from 2nm to 8nm. An in-house sp3d5s* empirical tight-binding model with spin-orbit coupling is used to calculate InP, GaAs, GaSb, and InSb DG-UTB band structures. The sp3d5s* tight-binding parameters are taken from Refs. [5-6]. Two surface orientations (111) and (100) are taken into account and their corresponding transport directions are [1-10] and [110], respectively. The energy dependent density of states and electron velocity are then extracted from the energy dispersion. After that an in-house top-of-the-barrier (TOB) model is used to study the ballistic performance. Notice that the injection velocity is essentially an average value weighted by the carrier density. Also the gate capacitance Cg in TOB is evaluated from series connections of two capacitors, insulator and quantum capacitance. The quantum capacitance depends on DOS and its formula is derived from Ref.[7]. This theoretical study mainly focuses on the band structure effects. Therefore source-to-drain and band-to-band tunneling are not taken into account in this work. The performance comparison is based on the same drain voltage Vd=0.8v and off-state current, Ioff=0.1μA/um. EOT=1nm is used in the simulation.

To validate the model used in this work, a comparison of the DOS in GaSb and GaAs UTB FETs with literature [2] is made. As shown in fig.1, the simulated DOS of GaSb and GaAs UTB FETs with (100) and (111) surface orientations are in good agreement with the literature results.

III. SURFACE ORIENTATION EFFECTS

Fig.2 illustrates (111) surface orientation band structures of InP, GaAs, GaSb and InSb UTB FETs with 4nm body thickness. At the Brillouin zone center, GaSb and GaAs have multiple subbands and most of them are originally from bulk L-valleys [2] leading to a higher DOS with respective to InP and InSb FETs. Since the energy separations between Γ- and L-valley minimum in GaSb and GaAs UTB FETs are quite small (28meV for GaSb and 241.3meV for GaAs UTB 4nm), this causes their multiple subbands at Γ-point. For (100) surface orientation, each UTB band structure is shown in fig.4. As can be seen from fig.2 and fig.4, GaSb and GaAs have many subbands at Γ-valley compared to those in InP and InSb for (111) and (100) surface orientations. Therefore, the DOS of GaSb and GaAs is larger than that in InP and InSb as shown in

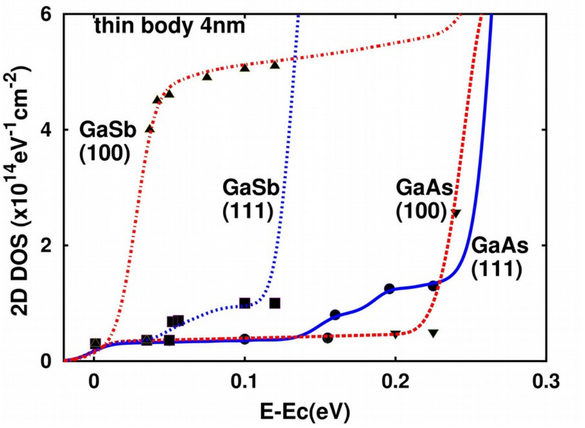

Fig.1 Density of states of GaSb and GaAs UTB FETs with (111) and (100) surface orientations. Solid upward triangle, square, circle, and downward triangle denote GaSb (100), GaSb (111), GaAs (111), and GaAs (100) UTB literature results from Ref.[2].

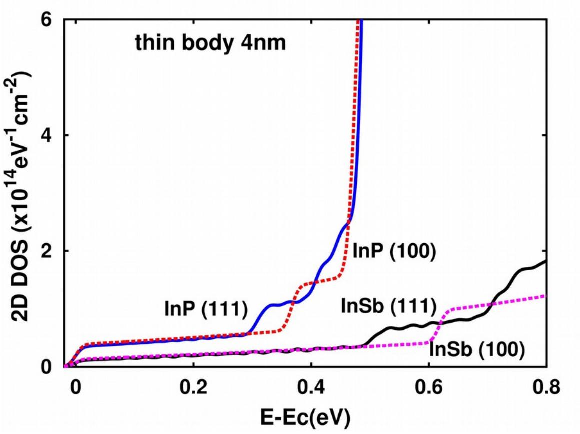

Fig.3 Density of states of InP and InSb UTB FETs with (111) and (100) surface orientations.

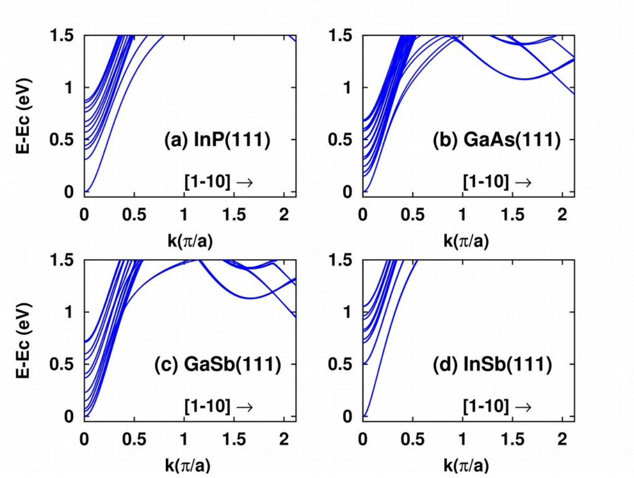

Fig.2 Band structures for (a) InP, (b) GaAs, (c) GaSb, (d) InSb thin body 4nm with (111) surface orientation and [1-10] transport direction.

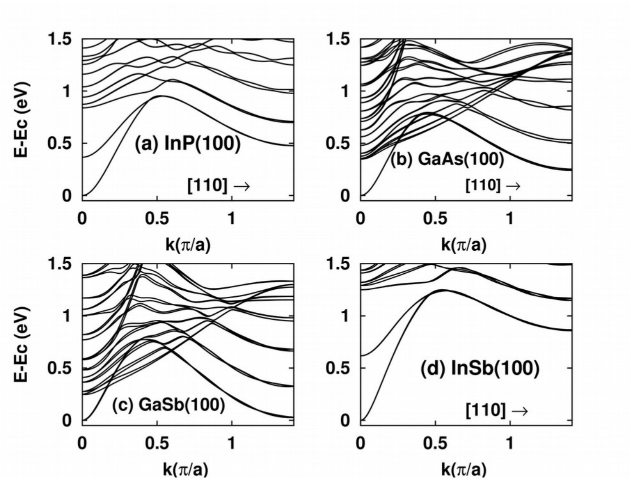

Fig.4 Band structures for (a) InP, (b) GaAs, (c) GaSb, (d) InSb thin body 4nm with (100) surface orientation and [110] transport direction.

fig.1 and fig.3. The impact of surface orientation on each UTB material will be discussed as follows.

A. InP

In fig. 3, the DOS of (111) InP is quite close to that in (100) for low energy but the (100) surface along [110] transport direction flattens its energy dispersion as shown in fig.5. Therefore, in fig.6 the carrier density in (100) InP is larger than that in (111) surface. Fig. 7 shows the injection velocity as a function of carrier density, Ninv. As can be seen in fig.7, the magnitude of the injection velocity in (100) InP gets closer to the one in (111) surface. Consequently, the Ion of (100) InP UTB FET is larger than that in (111) as shown in fig.8. Compared to silicon ballistic performance, for example, the Ion of a (100) InP FET with body thickness of 2nm is 1.51 times that of an unstrained-Si FET.

B. GaAs

In fig.1, since the DOS of (111) GaAs is larger than that in (100) surface, the carrier density of (111) surface is larger than

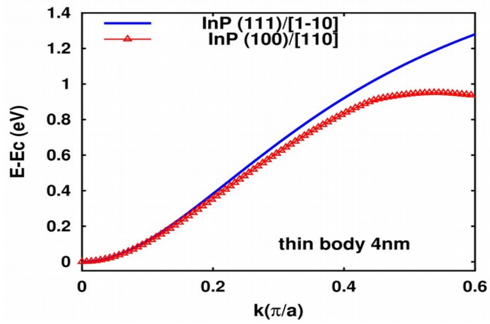

Fig.5 The first subband of InP UTB (100) surface has more flattened energy dispersion than that in InP UTB (111) surface.

that in (100) as shown in fig.6. However, the Ion of (100) GaAs is larger than (111) GaAs Ion as can be seen from fig.8 because the (100) injection velocity is greater than (111) injection velocity as shown in fig.7. Hence the injection velocity and

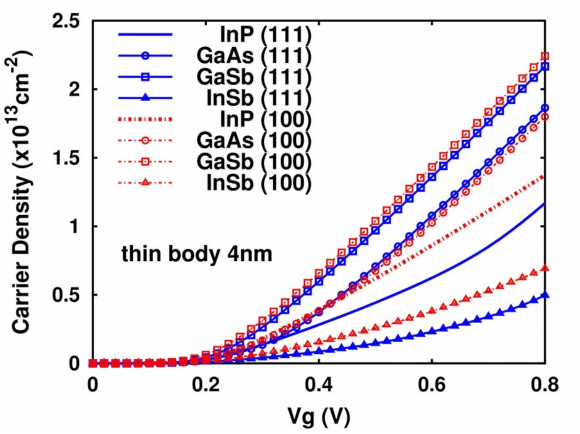

Fig.6 Carrier density of UTB FETs for (111)/[1-10] and (100)/[110] orientations with body thickness of 4nm.

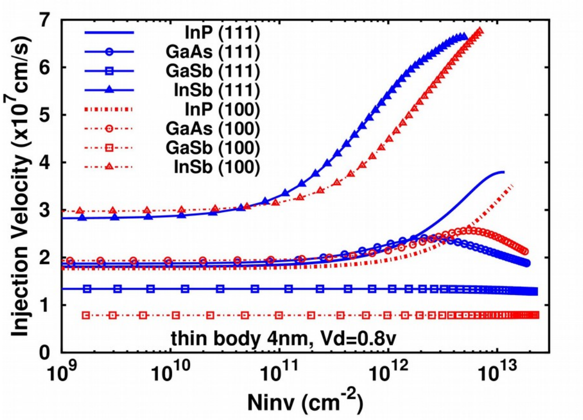

Fig.7 Injection velocity as a function of carrier density, Ninv, for (111)/[1-10] and (100)/[110] orientations with body thickness of 4nm.

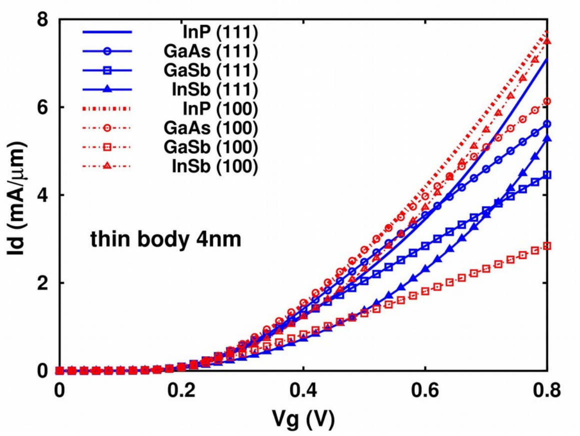

Fig.8 Drain current of UTB FETs for (111)/[1-10] and (100)/[110] orientations with body thickness of 4nm.

DOS impact on Ion simultaneously but the injection velocity seems to dominate in GaAs UTB FET.

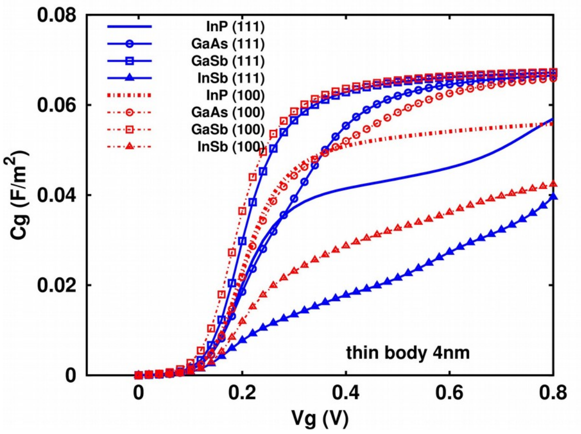

Fig.9 Gate capacitance of UTB FETs for (111)/[1-10] and (100)/[110] orientations with body thickness of 4nm.

C. GaSb

In fig.4(c), the energy separation of (100) GaSb UTB between its Brillouin zone edge and zone center minimum is quite small. As a result, the carriers are able to populate to the zone edge valleys easily. Thus (100) GaSb DOS increases quickly in small energy as shown in fig.1. Fig.6 shows that the corresponding (100) GaSb UTB carrier density is larger than that in (111) GaSb. However, (100) GaSb UTB has larger effective mass at the Brillouin zone edge resulting in degradation of its injection velocity as shown in fig.7. Therefore in fig.8 the Ion of (111) GaSb UTB is larger than that in (100) GaSb.

D. InSb

Similar to InP UTB, the Ion of (100) InSb UTB is greater than that of (111) surface due to the flattened energy dispersion in (100) surface. In addition, InSb UTB has the lightest Γ-valley effective mass so that its injection velocity is the greatest one as shown in fig.7.

The simulated III-V materials, in general, can be separated into two groups. One has only a few of degenerate subbands at the Brillouin zone center such as InP and InSb UTB FETs. Another group like GaSb and GaAs UTB FETs in (111) surface has DOS benefits resulting from its multiple subbands at the Brillouin zone center. However, as can be seen in fig. 7, the injection velocity degradation of GaSb and GaAs UTB FETs occurs earlier than the velocity degradation of InP and InSb UTB FETs, which indicates their transport degradation arising from the heavy effective mass at the Brillouin zone edge. For InP and InSb UTB FETs, as gate bias further increases, the injection velocity increases as shown in fig.7. Therefore, the drain current of InP is larger than that in GaSb and GaAs UTB FETs.

Fig.9 shows the gate capacitance for different UTB materials. This plot also reflects these two types of materials. The gate capacitance of GaSb and GaAs UTB FETs abruptly increases and then becomes saturated due to their large charge density. On the other hand, the gate capacitance of InP and InSb UTB FETs gradually increases as the gate bias increases due to their small charge density.

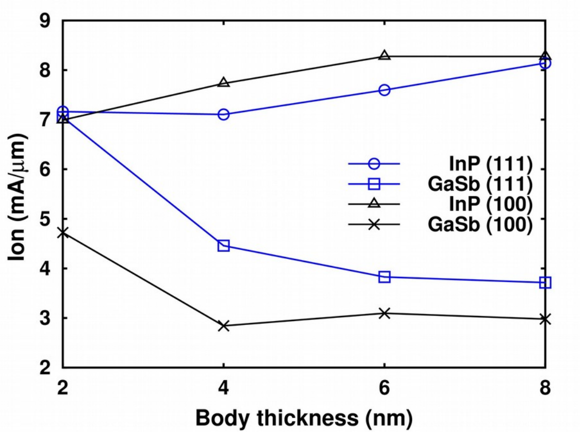

Fig.10 Comparison of on-state current Ion at Vd=Vg=0.8v among InP and GaSb UTB FETs with two surface orientations (111) and (100).

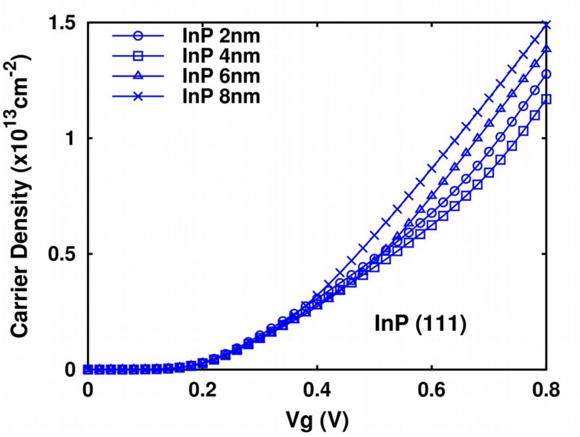

Fig.11 Carrier density vs. Vg plots for InP (111) UTB FETs with body thickness of 2nm to 8nm.

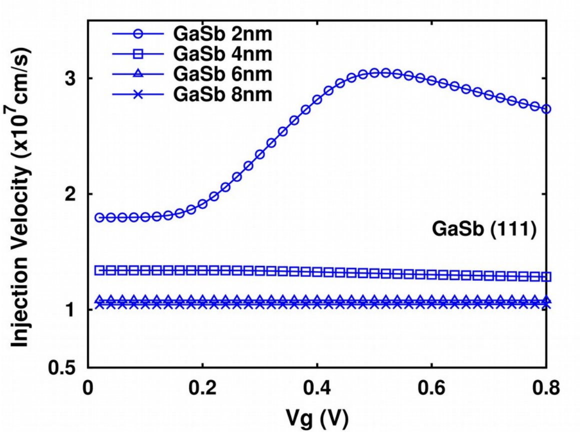

Fig.12 Injection velocity vs. Vg plots for GaSb (111) UTB FETs with body thickness of 2nm to 8nm.

IV. UTB THICKNESS EFFECTS

The body thickness effects on Ion are shown in fig.10. For InP UTB FETs, no mater what surface orientation is, the Ion increases as the body thickness increases. On the contrary, a GaSb UTB FET increases the Ion as its body thickness decreases. Fig. 11 indicates that the carrier density of InP UTB FETs, in principle, increases as the body thickness increases. Since the body thickness increases, more subbands drop to lower energy levels leading to an increase of DOS and carrier density. Fig.12 shows that an increase of the injection velocity causes the Ion improvement in a thinner GaSb UTB. This is because thinner body thickness increases the energy band separation between each subband resulting in an increase of the injection velocity. Therefore, the DOS and injection velocity are two major factors to determine InP and GaSb UTB body thickness effects, respectively.

V. CONCLUSIONS

In this article, the ballistic performance comparisons of III-V UTB FETs including InP, GaAs, GaSb, and InSb materials have been studied from the surface orientation and body thickness perspectives. It further explores the ballistic performance root cause in terms of the UTB DOS and injection velocity. From the surface orientation point of view, (111) surface yields the DOS benefits due to the multiple subbands at Γ-point. However, the ballistic Ion in (100) is greater than that in (111) surface except that in GaSb UTB. From the material point of view, InP yields better ballistic performance due to its high injection velocity. For body thickness effects, thicker body thickness in InP UTB provides more low energy subbands for carrier occupancy thereby leading to an increase of the carrier density and its Ion. However, a thinner body thickness value in GaSb UTB increases the energy separation between each subband resulting in an increase of the injection velocity and Ion.

REFERENCES

[1] J. A. del Alamo, “Nanometre-scale electronics with III-V compound semiconductors,” Nature, vol. 479, pp. 317-323, Nov. 2011.

[2] R. Kim, T. Rakshit, R. Kotlyar, S. Hasan, and C. E. Weber, “Effects of Surface Orientation on the Performance of Idealized III-V Thin-Body Ballistic n-MOSFETs,” IEEE Electron Device Lett., vol. 32, no. 6, pp. 746-748, Jun. 2011.

[3] M. Luisier, “Performance Comparison of GaSb, Strained-Si, and InGaAs Double-Gate Ultrathin-Body n-FETs,” IEEE Electron Device Lett., vol. 32, no. 12, pp. 1686-1688, Dec. 2011.

[4] Y. Guo, X. Zhang, K. L. Low, K.-T. Lam, Y.-C. Yeo, and G. Liang, “Effect of body Thickness on the Electrical Performance of Ballistic n-Channel GaSb Double-Gate Ultrathin-Body Transistor,” IEEE Electron Devices, vol. 62, no. 3, pp. 788-794, Mar. 2015.

[5] T. B.Boykin, G. Klimeck, R. C. Bowen, and F. Oyafuso, “Diagonal parameter shifts due to nearest-neighbor displacements in empirical tight-binding theory,” Phys. Rev. B. Condens. Matter, vol. 66, no. 12, p. 125207, 2002.

[6] J.-M. Jancu, R. Scholz, F. Beltram, and F. Bassani, “Empirical spds* tight-binding calculation for cubic semiconductors: General method and material parameters,” Phys. Rev. B. Condens. Matter, vol. 57, no. 11, pp. 6493-6507, Mar. 1998.

[7] A. Rahman, J. Guo, S. Datta, and M. S. Lundstrom, “Theory of ballistic Nanotransistors,” IEEE Electron Devices, vol. 50, no. 9, pp. 1853-1864, Sept. 2003.